Article

Electron Transfer within 2,7-Dinitronaphthalene Radical Anion

Stephen F. Nelsen, Michael N. Weaver, Asgeir E. Konradsson, Joo P. Telo, and Timothy Clark

J. Am. Chem. Soc., **2004**, 126 (47), 15431-15438• DOI: 10.1021/ja046566v • Publication Date (Web): 09 November 2004

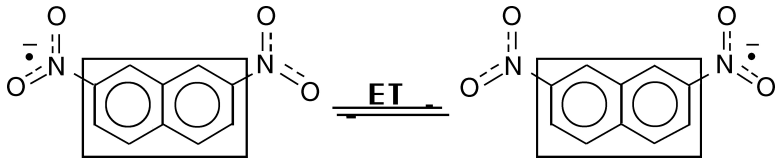

More About This Article

Additional resources and features associated with this article are available within the HTML version:

- Supporting Information
- Links to the 4 articles that cite this article, as of the time of this article download
- Access to high resolution figures
- Links to articles and content related to this article
- Copyright permission to reproduce figures and/or text from this article

View the Full Text HTML

J|A|C|S
ARTICLES
Published on Web 11/09/2004

Electron Transfer within 2,7-Dinitronaphthalene Radical Anion

Stephen F. Nelsen,*,† Michael N. Weaver,† Asgeir E. Konradsson,†
João P. Telo,*,‡ and Timothy Clark§

Contribution from the Department of Chemistry, University of Wisconsin, 1101 University Avenue, Madison, Wisconsin 53706-1396, Instituto Superior Técnico, Centro de Química Estrutural, Química Orgânica, Av. Rovisco Pais, 1049-001 Lisboa, Portugal, and Computer-Chemie-Centrum, Friedrich-Alexander-Universität Erlangen-Nürnberg, Nägelsbachstrasse 25, 91052 Erlangen, Germany

Received June 10, 2004; E-mail: nelsen@chem.wisc.edu; jptelo@ist.utl.pt

Abstract: The optical spectrum of 2,7-dinitronaphthalene radical anion generated by Na(Hg) reduction in acetonitrile containing a large excess of cryptand[2.2.2] exhibits a Hush-type intervalence charge-transfer band at 1070 nm, estimated to correspond to an off-diagonal matrix coupling element of 310 cm^{-1}. The interpolated rate constant for intramolecular electron transfer at 293 K measured by ESR between 225 and 320 K for this solution is 3.1(±0.2) × 10^9 s^{-1}. Rate constants estimated in two ways from the optical parameters using the Marcus−Hush assumption that the diabatic surfaces should be parabolae are 1.0 and 0.11 × 10^9 s^{-1}, and those using diabatic surfaces that fit the observed charge-transfer band are 9.6 and 3.4 × 10^9 s^{-1}, when used with an electron-transfer distance on the adiabatic surfaces of 6.42 Å. Similar measurements and comparisons were also carried out using dimethylformamide and butyronitrile as solvents. The success of simple, classical two-state Marcus−Hush theory precludes an electron-hopping mechanism. UHF calculations predict a planar unsymmetrical gas-phase structure for 1,3-dinitrobenzene radical anion but give serious spin contamination. Semiempirical AM1 calculations using singles excitation configuration interaction with an active space of 70 orbitals and the COSMO solvent model also give a planar unsymmetrical structure. These calculations make the internal vibrational component of the reorganization energy nearly constant, and much smaller than the solvent reorganizational component, and predict the transition energy to lie between that observed in acetonitrile (9360 cm^{-1}) and those observed in dimethylformamide (8100 cm^{-1}) and butyronitrile (8040 cm^{-1}).

Introduction

The title compound (**1**$^{\bullet-}$) has an unsymmetrical charge distribution and undergoes intramolecular electron transfer (ET) at a rate convenient to measure by ESR, and slightly slower than that of its single-ring analogue, *meta*-dinitrobenzene radical anion (**2**$^{\bullet-}$).

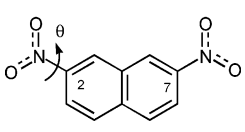

1

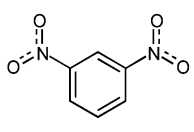
2

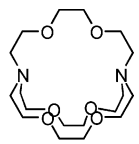
3

These radical anions and their analogues were among the first systems for which intramolecular ET reactions were studied in detail, using ESR, during a flurry of activity by several groups between 1960 and 1970.[1−8] More recently, the ET rate constants for these species generated either by electrochemical reduction or by photolysis have been measured more accurately using computer simulation of the entire ESR spectrum.[9,10] Hosoi, Mori,

† University of Wisconsin.
‡ Instituto Superior Técnico.
§ Friedrich-Alexander-Universität Erlangen-Nürnberg.

(1) (a) Ward, R. L. *J. Chem. Phys.* **1960**, *32*, 410. (b) Ward, R. L. *J. Am. Chem. Soc.* **1960**, *82*, 1296. (c) Ward, R. L. *J. Chem. Phys.* **1962**, *37*, 1405.
(2) (a) Maki, A. H.; Geske, D. H. *J. Chem. Phys.* **1960**, *33*, 825. (b) Maki, A. H.; Geske, D. H. *J. Am. Chem. Soc.* **1961**, *83*, 1852. (c) Harriman, J. E.; Maki, A. H. *J. Chem. Phys.* **1963**, *39*, 778.
(3) (a) Freed, J. H.; Rieger, P. H.; Fraenkel, G. K. *J. Chem. Phys.* **1962**, *37*, 1881. (b) Freed, J. H.; Fraenkel, G. K. *J. Chem. Phys.* **1963**, *39*, 326. (c) Rieger, P. H.; Fraenkel, G. K. *J. Chem. Phys.* **1963**, *39*, 609. (d) Bernal, I.; Fraenkel, G. K. *J. Am. Chem. Soc.* **1964**, *86*, 1671−1675. (e) Freed, J. H.; Fraenkel, G. K. *J. Chem. Phys.* **1964**, *41*, 699. (f) Fraenkel, G. K. *J. Phys. Chem.* **1967**, *71*, 139. (g) Faber, R. J.; Fraenkel, G. K. *J. Chem. Phys.* **1967**, *47*, 2462.
(4) (a) Geske, D. H.; Ragle, J. L.; Bambenek, M. A.; Balch, A. L. *J. Am. Chem. Soc.* **1964**, *86*, 987. (b) Gulick, W. M., Jr.; Geske, D. H. *J. Am. Chem. Soc.* **1965**, *87*, 4049. (c) Gulick, W. M., Jr.; Geiger, W. E., Jr.; Geske, D. H. *J. Am. Chem. Soc.* **1968**, *90*, 4218.
(5) Buley, A. L.; Norman, R. O. C. *Proc. Chem. Soc.* **1964**, 225.
(6) (a) Blandamer, M. J.; Gough, T. E.; Gross, J. M.; Symons, M. C. R. *J. Chem. Soc.* **1964**, 536. (b) Fox, W. M.; Gross, J. M.; Symons, M. C. R. *J. Chem. Soc. A* **1966**, 448. (c) Claxton, T. A.; Fox, W. M.; Symons, M. C. R. *Trans. Faraday Soc.* **1967**, *63*, 2570. (d) Symons, M. C. R. *J. Phys. Chem.* **1967**, *71*, 172.
(7) (a) Allendoerfer, R. D.; Rieger, P. H. *J. Am. Chem. Soc.* **1966**, *88*, 3711. (b) Allendoerfer, R. D.; Rieger, P. H. *J. Chem. Phys.* **1967**, *46*, 3410.
(8) (a) Gutch, C. J. W.; Waters, W. A. *J. Chem. Soc., Chem. Commun.* **1966**, 39. (b) Griffiths, W. E.; Longster, G. F.; Myatt, J.; Todd, P. F. *J. Chem. Soc. B* **1966**, 1130. (c) Griffiths, W. E.; Gutch, C. J. W.; Longster, G. F.; Myatt, J.; Todd, P. F. *J. Chem. Soc. B* **1968**, 785. (d) Gutch, J. W.; Waters, W. A.; Symons, M. C. R. *J. Chem. Soc. B* **1970**, 1261.
(9) (a) Grampp, G.; Shohoji, M. C. B. L.; Herold, B. J. *Ber. Bunsen-Ges. Phys. Chem.* **1989**, *93*, 580. (b) Grampp, G.; Shohoji, M. C. B. L.; Herold, B. J.; Steenken, S. *Ber. Bunsen-Ges. Phys. Chem.* **1990**, *94*, 1507. (c) Telo, J. P.; Shohoji, M. C. B. L.; Herold, B. J.; Grampp, G. *J. Chem. Soc., Faraday Trans.* **1992**, *88*, 47. (d) Telo, J. P.; Shohoji, M. C. B. L. *Ber. Bunsen-Ges. Phys. Chem.* **1994**, *98*, 172.
(10) Hosoi, H.; Mori, Y.; Masuda, Y. *Chem. Lett.* **1998**, 177.

and Masuda showed that ion-pairing significantly affects the ET rate constants even when the counterion is tetrabutylammonium, in rather polar solvents.[10] They found an order of magnitude larger ET rate constants for $\mathbf{2}^{\bullet-}$ generated using sodium amalgam reduction in the presence of an excess of cryptand[2.2.2] (**3**) in both acetonitrile and dimethylformamide, than Grampp and co-workers obtained.[9] The latter group used electrochemical reduction with tetrabutylammonium salts as supporting electrolyte, conditions that had been assumed to produce $\mathbf{2}^{\bullet-}$ lacking significant ion-pairing effects since the pioneering work of Geske and Maki.[2a]

It has been assumed from the beginning of work on these systems that the nitro groups of dinitroaromatic radical anions would be equivalent in the absence of perturbation by solvent and/or counterion. Dinitroaromatic radical anions were not perceived as intervalence compounds because this concept was only devised in the late 1960s with reference to transition-metal coordination compounds,[11] so there was no theoretical framework for the idea that localization of charge onto one of the nitro groups might occur spontaneously. Miller's group did important work on linear aryl-linked terminal diquinone radical anions in the early 1990s. Optical studies showed that charge localization into one naphthoquinone unit occurs for tetracene- and pentacenetetraones, and rate constants for intramolecular electron transfer between the naphthoquinone units were determined by ESR and compared with Marcus−Hush theory predictions.[12] In contrast, the 5−8 ring helicene analogues prepared by Katz, which have significant through-space overlap between the terminal quinone units, proved to be all delocalized.[13]

According to Marcus−Hush theory, localization of charge will occur when the off-diagonal matrix element that measures electronic interaction between the two charge-bearing units in the two-state model (the H_{ab} of Marcus−Hush theory) is less than half of the total vertical reorganization energy (the λ of Marcus−Hush theory).[11,14] The "non-Kekulé" substitution pattern of $\mathbf{1}^{\bullet-}$ and $\mathbf{2}^{\bullet-}$ ensures that H_{ab} is rather small, but so is λ, unless the geometries of the neutral and reduced nitro groups become significantly different. All interactions with solvent and counterion will increase λ and hence make charge localization more likely. Ion-pairing was invoked in early discussions as the cause of the charge localization observed,[1,2] but it was later pointed out that the nitro groups remain inequivalent in water, where ion-pairing should be too weak to cause charge localization.[8c] Hydrogen bonding lowers the rate constants for nitro group interconversion by about a factor of 1000, but the dissymmetry revealed by the ESR spectrum occurs in all solvents studied in detail, even in the absence of hydrogen bonding and ion-pairing. Introduction of ortho-substituents raises the barriers for nitro-group interconversion, which was interpreted as demonstrating that twisting occurs at one of the Ar−NO_2 bonds in the localized form. In the final paper on the subject for almost 20 years, Gutch, Waters, and Symons in 1970 invoked preferential solvent interaction with a reduced nitro group as being responsible for the charge localization.[8d] They also proposed that, because the delocalized species is the most stable in the gas phase, and solvent effects stabilize the species with charge localized on one nitro group, the delocalized species would be an intermediate in the ET reaction that equilibrates the nitro groups. We believe that this was the first postulation of an experimental system for which ET would proceed through what was called the "chemical mechanism" by Kosloff and Ratner in a 1990 review article on superexchange[15] (no examples shown to use such a mechanism were given), and more recently is being called an "electron hopping" mechanism.[16] In the Marcus−Hush two-state model, the symmetrical species is a transition state; concerted electron transfers to and from the bridge cause the overall process to be equivalent to one electron moving from one charge-bearing unit to the other without any intermediate. For the Marcus−Hush model to predict the ET rate constant accurately, the symmetrical state must lie substantially higher in energy than the charge-localized ground state.[15] The Marcus−Hush model predicts intramolecular rate constants accurately for intervalence bis(hydrazine) radical cations having benzene, naphthalene, and biphenyl bridges,[17] but the observed rate constant is on the order of 150 times faster than this model predicts when the 9,10-anthyryl bridge is present. It was argued from analysis of the optical spectrum that the symmetrically bridged species for this system is an excited state that lies too high in energy to cause a minimum to appear for the symmetrical species on the ground-state energy surface, but too low for the two-state model to be accurate.[18]

Results

In this work, we determined the ESR spectra of solutions of $\mathbf{1}^{\bullet-}$ generated using the sodium amalgam, cryptand **3** conditions of Hosoi, Mori, and Masuda[10] and obtained the optical spectra under the same conditions, to see how well the Marcus−Hush prediction of rate constant from the optical spectrum works. The ESR rate constants were determined at a range of temperatures by simulation of the ESR spectra using the program of Grampp et al.[9] The rate constants in CH_3CN and DMF we obtained for $\mathbf{2}^{\bullet-}$ are in good agreement with those reported by the Japanese group.[10] The experimental data determined for $\mathbf{1}^{\bullet-}$ are summarized in Table 1.

Figure 1 compares the near-IR spectra in DMF for 2,7-dinitronaphthalene $\mathbf{1}^{-}$ with that of its 2,6-isomer, $\mathbf{4}^{\bullet-}$. $\mathbf{4}^{\bullet-}$ has

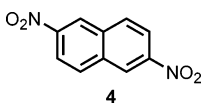

4

a substitution pattern leading to high H_{ab}, and as a result it is charge-delocalized and shows a narrow enough line width to

(11) (a) Robin, M.; Day, P. *Adv. Inorg. Radiochem.* **1967**, *10*, 247. (b) Hush, N. S. *Prog. Inorg. Chem.* **1967**, *8*, 391. (c) Hush, N. S. *Electrochim. Acta* **1968**, *13*, 1005.

(12) (a) Jozeriak, T. H.; Almlöf, J. E.; Feyereisen, M. W.; Miller, L. L. *J. Am. Chem. Soc.* **1989**, *111*, 4105. (b) Almlöf, J. E.; Feyereisen, M. Y.; Jozefiak, T. H.; Miller, L. L. *J. Am. Chem. Soc.* **1990**, *112*, 1206. (c) Rak, S. F.; Jozeriak, T. H.; Miller, L. L. *J. Org. Chem.* **1990**, *55*, 4794. (d) Rak, S. F.; Miller, L. L. *J. Am. Chem. Soc.* **1992**, *114*, 13887−94. (e) Liberko, C. A.; Rak, S. F.; Miller, L. L. *J. Org. Chem.* **1992**, *57*, 1379.

(13) (a) Yang, B.; Liu, L.; Katz, T. J.; Liberko, C. A.; Miller, L. L. *J. Am. Chem. Soc.* **1991**, *113*, 8993. (b) Liberko, C. A.; Miller, L. L.; Katz, T. J.; Liu, L. *J. Am. Chem. Soc.* **1993**, *115*, 2478.

(14) For reviews of Marcus theory, see: (a) Marcus, R. A.; Sutin, N. *Biochim. Biophys. Acta* **1985**, *811*, 265−322. (b) Sutin, N. *Prog. Inorg. Chem.* **1983**, *30*, 441−99.

(15) Kosloff, R.; Ratner, M. A. *Isr. J. Chem.* **1990**, *30*, 45.

(16) Jortner, J.; Bixon, M.; Langenbacher, T.; Michel-Beyerle, M. E. *Proc. Natl. Acad. Sci. U.S.A.* **1998**, *95*, 12759.

(17) (a) Nelsen, S. F.; Ismagilov, R. F.; Powell, D. R. *J. Am. Chem. Soc.* **1997**, *119*, 10213. (b) Nelsen, S. F.; Ismagilov, R. F.; Trieber, D. A., II. *Science* **1997**, *278*, 846. (c) Nelsen, S. F.; Ismagilov, R. F.; Gentile, K. E.; Powell, D. R. *J. Am. Chem. Soc.* **1999**, *121*, 7108.

(18) Nelsen, S. F.; Ismagilov, R. F.; Powell, D. R. *J. Am. Chem. Soc.* **1998**, *120*, 1924.

Table 1. Summary of ESR Determination of the Intramolecular ET Rate Constant for 2,7-Dinitronaphthalene Radical Anion ($\mathbf{1}^{\bullet-}$)

solvent	CH_3CN	DMF	PrCN
T-range studied (K)	225−320	220−325	230−305
$k_{ESR,293}$ (10^9 s^{-1})[a]	3.1 ± 0.2	7.1 ± 0.5	7.1 ± 0.5
$\Delta G_{293}^{\ddagger}$ (kcal/mol)[a,b]	4.42 ± 0.04	3.92 ± 0.04	4.08 ± 0.06
$\Delta H^{\ddagger}$ (kcal/mol)[a,b]	4.4 ± 0.24	3.1 ± 0.26	3.4 ± 0.46
$\Delta S^{\ddagger}$ (cal K^{-1} mol^{-1})[a,b]	0.1 ± 0.9	−2.9 ± 1.0	−2.4 ± 1.7

[a] Interpolated to 293 K. [b] Range quoted reflects statistical error only.

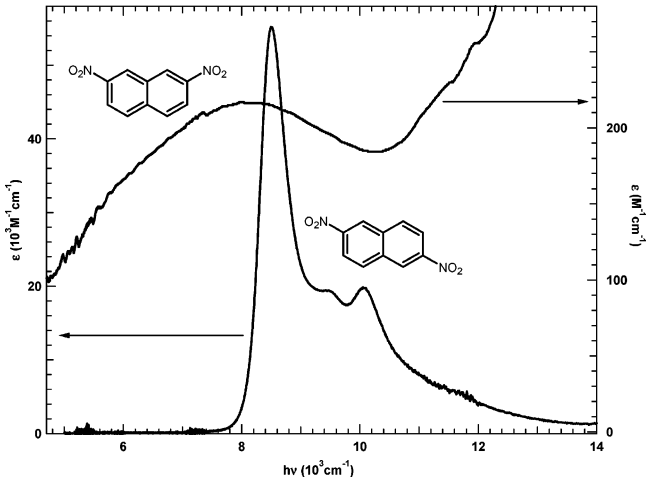

Figure 1. Comparison of optical spectra in DMF for the delocalized 2,6-dinitronaphthalene radical anion with that for the localized 2,7-isomer.

have vibrational fine structure. In contrast, $\mathbf{1}^{\bullet-}$, which has a non-Kekulé substitution pattern that leads to small H_{ab}, has the very broad, nearly Gaussian band shape expected for a localized intervalence compound. Although the band maxima have nearly the same energy for these isomers, their interpretation is quite different. According to two-state theory, the band maximum for delocalized intervalence compounds represents twice the electronic coupling, $2H_{ab}$, as discussed recently for $\mathbf{4}^{\bullet-}$ and five of its analogues that are also delocalized.[19] In contrast, the band maximum for $\mathbf{1}^{\bullet-}$ is a measure of its vertical reorganization energy, λ, and its ϵ value is related to H_{ab} and is a small fraction of that for $\mathbf{4}^{\bullet-}$. Although λ is not directly obtained from the optical spectrum of a delocalized intervalence compound like $\mathbf{4}^{\bullet-}$, the vibrational fine structure present in the spectrum allows estimation of both the internal vibrational component λ_v at about 790 cm^{-1} and the solvent-reorganization energy λ_s at about 510 cm^{-1}.[20] Because λ_s is only supposed to depend on molecular size, the values for these isomers should be rather similar, so λ_v must be approximately 9.6 times larger for the localized $\mathbf{1}^{\bullet-}$ than it is for the delocalized $\mathbf{4}^{\bullet-}$.

The optical parameters relating to the ET rate constant prediction for $\mathbf{1}^{\bullet-}$ were determined by fitting the observed spectra as the sum of an intervalence charge-transfer band having the shape expected for diabatic surfaces with a quartic as well as a parabolic component,[17] and a sufficient number of Gaussians for higher energy bands to maintain fit to the observed spectrum until the intervalence band has dropped to a negligibly small ϵ value, as was recently used for fitting intervalence bis(hydrazine) optical spectra.[21] See Figure 2 for the fit in

Table 2. Summary of Intervalence Charge-Transfer Band Optical Data for 2,7-Dinitronaphthalene Radical Anion ($\mathbf{1}^{\bullet-}$)

solvent	CH_3CN	DMF	PrCN
$E_a = \lambda$ (cm^{-1})[a]	9360	8100	8040
ϵ (M^{-1} cm^{-1})	177	215	177
$\Delta\nu_{1/2}$ (cm^{-1})	6750	7000	6990
μ_{12} (D)[b]	1.12,[c] 1.04[d]	1.35,[c] 1.24[d]	1.23,[c] 1.14[d]
H_{ab} (cm^{-1})[b]	310,[c] 320[d]	310,[c] 320[d]	290,[c] 300[d]
quartic C	0.35	0.5	0.5

[a] Band maximum. [b] Calculated using the Chacko refractive index correction (see text) and d_{ab} = 6.44 Å. [c] Estimated using the Hush approximation, that is, $H_{ab} = 0.0206N(\epsilon\Delta\nu_{1/2}\lambda)^{1/2}/d_{ab}$. [d] Estimated using Liptay's method.[24]

acetonitrile. Our calculation of H_{ab} employed the refractive index (n) correction $N = 3(n)^{1/2}/(n^2 + 2)$, introduced by Chacko and recently employed for this purpose by Gould and co-workers.[22] Calculation of H_{ab} requires the distance that charge moves during the ET, d_{ab}. The distance between the nitrogens in AM1 calculations of $\mathbf{1}^{\bullet-}$ having both charge-localized and delocalized structures is 7.42−7.43 Å. Because charge is obviously partially delocalized into the naphthalene ring, d_{12} should be somewhat shorter than this distance.[23] The d_{ab} used here was 6.44 Å in all three solvents, obtained using the d_{12} value of 6.42 Å, calculated by AM1 from the dipole moment of AUHF charge-localized structures, combined with the transition dipole μ_{12} as discussed in detail recently.[23] Table 2 includes both H_{ab} values calculated using the Hush Gaussian approximation ($H_{ab} = 0.0206N(\epsilon\Delta\nu_{1/2}\lambda)^{1/2}/d_{ab}$) and that using Liptay's equation[24] employing the integral of the $\epsilon/h\nu$ versus $h\nu$ plot (also with the same refractive index correction); the two estimates do not differ significantly in this case. The H_{ab} obtained using the calculated ET distance is 15% larger than that if the distance between the nitro nitrogens were used as d_{ab}, as has been traditional for such estimates.

The above Marcus−Hush analysis assumes a superexchange process,[15] that is, that the longest wavelength band for $\mathbf{1}^{\bullet-}$ corresponds to excitation between states having charge mostly localized on each nitro group, symbolized $^{-}$**O$_2$N-Naphth-NO$_2$** → **O$_2$N-Naphth-NO$_2^{-}$**. Another possibility in principle is that this band would be a "bridge reduction" band, corresponding to transfer of the electron to the naphthalene ring, $^{-}$**O$_2$N-Naphth-NO$_2$** → **O$_2$N-Naphth^{-}-NO$_2$**. The "bridge oxidation" analogue of such a band, $^{+}$**Hy-Anth-Hy** → **Hy-Anth^{+}-Hy**, is the lowest energy one for the 9,10-bis(hydrazine)-substituted anthracene radical cation.[18] We believe that the possibility that the long wavelength band for $\mathbf{1}^{\bullet-}$ corresponds to bridge reduction is ruled out by the lowest energy band for the benzene derivative $\mathbf{2}^{\bullet-}$ being centered at 8320 cm^{-1} in acetonitrile, 1030 cm^{-1} lower in energy than that for the naphthalene derivative $\mathbf{1}^{\bullet-}$. Cyclic voltammetry data in DMF show that it is 80 cm^{-1} easier to reduce 2-nitronaphthalene than nitrobenzene, so we would predict the opposite trend if the bands corresponded to bridge reduction.[25] The trend is correct for the nitro-to-nitro charge transfer to which we assign the bands. The smaller, benzene-bridged system has a band at lower energy, consistent

(19) Nelsen, S. F. Telo, J. P.; Konradsson, A. E.; Weaver, M. N. *J. Am. Chem. Soc.* **2003**, *125*, 12493.
(20) We estimate λ_s for 2,6-dinitronaphthalene radical anion from the band broadening necessary to obtain fit, the Γ parameter of the band fit on page S6 of the Supporting Information, see p S10.
(21) Nelsen, S. F.; Trieber, D. A., II.; Ismagilov, R. F.; Teki, Y. *J. Am. Chem. Soc.* **2001**, *123*, 5684.
(22) (a) Chako, N. Q. *J. Chem. Phys.* **1934**, *2*, 644. (b) Gould, I. R.; Young, R. H.; Mueller, L. J.; Albrecht, A. C.; Farid, S. *J. Am. Chem. Soc.* **1994**, *116*, 8188.
(23) Nelsen, S. F.; Newton, M. *J. Phys. Chem. A* **2000**, *104*, 10023.
(24) Liptay, W. *Angew. Chem., Int. Ed. Engl.* **1969**, *8*, 177.

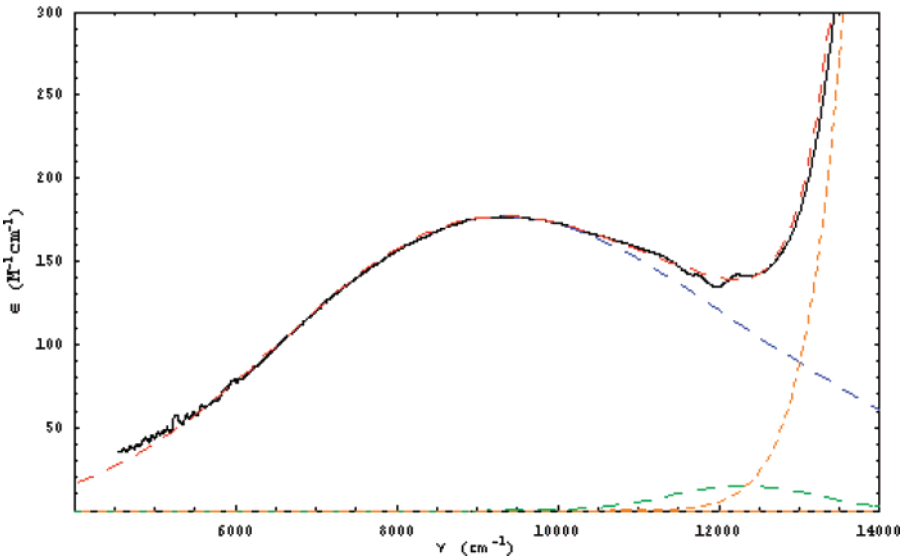

Figure 2. Experimental optical spectrum for **1**•− in acetonitrile (solid line) with superimposed broken lines for the quartic fit to the intervalence band, two Gaussian bands at higher energy, and the sum of the three bands, which mostly overlays with the experimental spectrum.

Table 3. Comparison of Optical with ESR Barriers and Rate Constants for **1**•−

solvent	CH_3CN	DMF	PrCN
$\Delta G_{ESR}^{\ddagger}(293)^a$	4.4	3.9	4.1
$\Delta G_{par}{}^{*a,b}$	5.8	4.9	5.0
$k_{LD}(par)^{c,d}$	1.0(0.32)	5.4(0.76)	4.3(0.78)
$\kappa_{el}{}^e$	0.37	0.40	0.35
$k_\kappa(par)^{c,f}$	0.36(0.11)	2.0(0.27)	1.7(0.31)
$\Delta G_{quar}{}^{*a,f,g}$	4.5	3.5	3.5
$k_{LD}(quar)^{c,d,g}$	9.6(3.1)	65(9.2)	51(9.3)
$k_\kappa(quar)^{c,f,g}$	3.4(1.1)	24(3.3)	20(3.6)

[a] Unit, kcal/mol. [b] Calculated using the Marcus−Hush assumption of parabolic diabatic surfaces, so $\Delta G^* = \lambda/4 - H_{ab} + H_{ab}{}^2/\lambda$. [c] Unit: 10^9 s^{-1}. [d] Calculated using eq 1 and the ΔG^* value indicated. Number in parentheses is k_{calc}/k_{ESR}. [e] Calculated as discussed in ref 17a using $h\nu_v$ = 1500 cm^{-1}. [f] Calculated using eq 2 and the ΔG^* value indicated. Number in parentheses is k_{calc}/k_{ESR}. [g] Calculated from the quartic-adjusted energy surfaces obtained from fitting the bands.

with the more rapid intramolecular ET between the nitro groups that is observed by ESR.[8d,9c]

Discussion

A comparison between the ESR rate constants and barriers and those predicted from the optical spectrum is given in Table 3. As shown in Table 2, slightly larger H_{ab} values were obtained using the Liptay equation for calculating H_{ab}, but the increases in rate constant that would be obtained in Table 3 by using the large H_{ab} values are not significant because there is much greater uncertainty in what to use for d_{ab}. We present two ways of converting the optically derived ET parameters into predicted rate constants for ET. We previously discussed using the simple Levich and Dogonadze equation for both intermolecular[26] and intramolecular reactions.[18] We have modified it for use in the "less nonadiabatic" region by employing ΔG^* instead of $\lambda/4$ in the exponential term; that is, we use eq 1 to calculate one type of rate constant from the optical data.

$$k_{LD} = 2\pi/\tilde{N}(4\pi RT)^{-1/2}\cdot H_{ab}{}^2/(\lambda)^{1/2}\cdot\exp[-\Delta G^*/RT] \quad (1)$$

We also used a different expression, in which an electronic transmission coefficient k_{el} has been added to an adiabatic rate constant expression, allowing it to be used in the "less than adiabatic" region, eq 2,[14b] although using it requires additional assumptions.

$$k_\kappa = \kappa_{el}ch\nu_v\cdot(\lambda_v/\lambda)^{1/2}\cdot\exp[-\Delta G^*/RT] \quad (2)$$

We used an estimated $h\nu_v$ value of 1500 cm^{-1}, as commonly used for aromatic systems,[11b,14] and λ_v of 6.2 kcal/mol, close to the value calculated (see below). As shown in Table 3, the calculated-to-observed rate ratio is smaller using eq 2 than using eq 1. Two estimates of ΔG^* were used. Using the original Marcus−Hush classical two-state model with parabolic diabatic surfaces makes $\Delta G_{par}{}^* = \lambda/4 - H_{ab} + (H_{ab})^2/\lambda$.[3b] The rate constants calculated using eqs 1 and 2 with $\Delta G_{par}{}^*$ are smaller than those observed by ESR (k_{calc}/k_{ESR} between 0.2 and 0.8). However, the IV-CT bands observed are broader than the values that would result from parabolic diabatic surfaces. Best fit to the observed spectra gave quartic parameter C values of 0.35 in acetonitrile and 0.5 in DMF and butyronitrile (see Table 1). Diabatic surface crossover occurs at a smaller value than $\lambda/4$ as C increases,[17a,b] producing the $\Delta G_{quar}{}^*$ and k(quar) values shown in Table 2. The rate constants predicted using optically derived ET parameters are somewhat larger than the observed ones when a barrier consistent with the observed intervalence bandwidth is employed, but both k_{LD}(quar) and k_κ(quar) are within an order of magnitude of k_{ESR}. The main point demonstrated by Table 3 is that the optical spectra produce barriers that predict the rate constants surprisingly well by assuming that the ET has a superexchange mechanism. The optical data for **1**•− were only recorded at 293 K, but in previous studies of bis(hydrazines) as a function of temperature it has been found that, although optically derived λ, ϵ, and $\Delta\nu_{1/2}$ all change slightly, the ΔG^* obtained was constant within experimental error.[17c] If a constant ΔG^* is also used for **1**•−, the variations of k_{et} with temperature that are predicted using both eqs 1 and

(25) (a) Bock, H.; Lechner-Knoblauch. *Z. Naturforsch.* **1985**, *40b*, 1463. (b) Surprisingly to us, **2** is 560 cm^{-1} harder to reduce than **1**.[21a] Because an unpaired electron is already present in **1**•− and **2**•−, we suggest that it is the reduction potentials of the mononitro compounds quoted in the text that are most relevant to relative positions expected for their bridge reduction bands.

(26) Nelsen, S. F.; Trieber, D. A., II; Nagy, M. A.; Konradsson, A.; Halfen, D. T., Splan, K. A.; Pladziewicz, J. R. *J. Am. Chem. Soc.* **2000**, *122*, 5940.

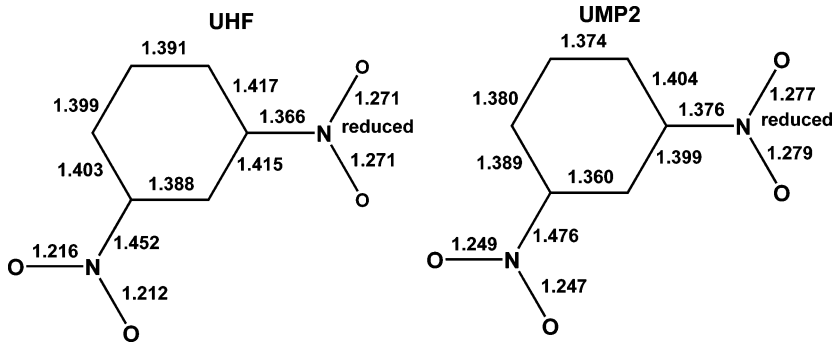

Figure 3. Bond lengths (Å) for UHF and UMP2 structures of $\mathbf{2}^{\bullet-}$ at the 6-31+G(d) level.

2 are rather close to those observed experimentally. For example, the $\Delta S^{\ddagger}$ value predicted from the optical data in CH_3CN using eq 1 is 1.6 cal K^{-1} mol^{-1}, and those for DMF and butyronitrile are very similar (1.8 and 1.4 cal K^{-1} mol^{-1}, respectively).

We conclude that, in contrast to our initial expectation, the simple two-state Marcus−Hush model predicts the ET rate constant for $\mathbf{1}^{\bullet-}$ rather well. We had not expected this because, as pointed out above, a small energy difference between the localized and delocalized states leads to this model predicting rate constants that are substantially too small.[18] These results indicate that, for these systems, the symmetrical ring-centered radical anion that people have assumed would be an intermediate in these systems is not an intermediate in the ET process, despite it being predicted to be the most stable species in previously published gas-phase calculations.

Calculations

We have used calculations to try to understand why the unexpected result of $\mathbf{1}^{\bullet-}$ having intramolecular ET that is predicted well by the Marcus−Hush two-state model occurs, and also to more accurately estimate the electron-transfer distance d_{ab} that was used to calculate H_{ab}. Large basis set calculations were carried out on the smaller system, $\mathbf{2}^{\bullet-}$, for reasons of economy. Although density functional theory (DFT) calculations are excellent for most radical ions, and are especially successful for predicting ESR spectra,[27] presently available functionals prove totally incapable of properly obtaining the difference in geometry between the oxidized and reduced hydrazine units of intervalence bis(hydrazine) radical cations[28] and are useless for considering intermolecular ET in intervalence compounds. We have therefore not tried to use DFT calculations to understand intervalence dinitro anions. Rather surprisingly to us, because people have assumed that the gas-phase structure is symmetrical since 1960, a UHF/6-31+G(d) calculation on $\mathbf{2}^{\bullet-}$ gives an unsymmetrical but essentially planar gas-phase structure that is 6.7 kcal/mol more stable than the symmetrical structure.[29,30] The reduced CNO_2 fragment is calculated to have a charge of −0.66, and the other CNO_2 fragment is calculated to have a charge of −0.35.[31] Obtaining an unsymmetrical structure is not simply an artifact of having no electron correlation, because a UMP2 calculation using the same basis set produces a rather similar structure (see Figure 3),[32] nor of having diffuse functions, because the UHF/6-31G(d) calculation that lacks the diffuse functions gives a very similar localized structure that is 6.9 kcal/mol more stable than the C_{2v} structure. A Natural Resonance Theory analysis[33] gives the valence bond resonance forms for the UHF/6-31+G(d) calculation making the largest contributions to the structure as those shown in Figure 4, rationalizing the shorter CN bond length for the reduced than the neutral NO_2 unit (by 0.086 Å), and the longer NO bond length (by 0.06 Å). For the UMP2 calculation, these differences are $\Delta CN = 0.100$ Å and $\Delta NO = 0.029$ Å. A second unsymmetrical structure lying 1.3 kcal/mol above that shown in Figure 3 was also obtained, see Figure 4. The NBO analysis shows that these structures differ in whether the shorter NO bond in the β spin set (that with more N═O character) is eclipsed with a shorter ring C−C bond (as the reduced nitrogen in the more stable isomer) or with the longer C−C bond (as the reduced nitrogen in the less stable isomer). These structural differences are reminiscent of those for the rotamers of *m*-xylene,[33c] where the rotamer with the CH bond eclipsed with the shorter bond (C_1C_2, closer to C═C) is about 2 kcal/mol

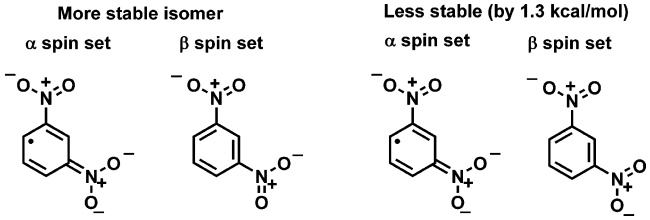

Figure 4. Valence structures obtained from a Natural Resonance Theory analysis of the unsymmetrical isomers of $\mathbf{2}^{-}$.

(27) (a) Batra, R.; Giese, B.; Spichty, M.; Gescheidt, G.; Houk, K. N. *J. Phys. Chem.* **1996**, *100*, 18371. (b) Bally, T.; Borden, W. T. In *Reviews in Computational Chemistry*; Lipkowitz, K. B., Boyd, D. B., Eds.; Wiley−VCH: New York, 1999; Vol. 13, p 1.

(28) Blomgren, F.; Larsson, S.; Nelsen, S. F. *J. Comput. Chem.* **2001**, *22*, 655.

(29) We thank Prof. Frank Weinhold (U. W. Madison) for pointing these unsymmetrical structures out to us and doing the NBO calculations.

(30) Frisch, M. J.; Trucks, G. W.; Schlegel, H. B.; Scuseria, G. E.; Robb, M. A.; Cheeseman, J. R.; Zakrzewski, V. G.; Montgomery, J. A., Jr.; Stratmann, R. E.; Burant, J. C.; Dapprich, S.; Millam, J. M.; Daniels, A. D.; Kudin, K. N.; Strain, M. C.; Farkas, O.; Tomasi, J.; Barone, V.; Cossi, M.; Cammi, R.; Mennucci, B.; Pomelli, C.; Adamo, C.; Clifford, S.; Ochterski, J.; Petersson, G. A.; Ayala, P. Y.; Cui, Q.; Morokuma, K.; Malick, D. K.; Rabuck, A. D.; Raghavachari, K.; Foresman, J. B.; Cioslowski, J.; Ortiz, J. V.; Baboul, A. G.; Stefanov, B. B.; Liu, G.; Liashenko, A.; Piskorz, P.; Komaromi, I.; Gomperts, R.; Martin, R. L.; Fox, D. J.; Keith, T.; Al-Laham, M. A.; Peng, C. Y.; Nanayakkara, A.; Gonzalez, C.; Challacombe, M.; Gill, P. M. W.; Johnson, B.; Chen, W.; Wong, M. W.; Andres, J. L.; Gonzalez, C.; Head-Gordon, M.; Replogle, E. S.; Pople, J. A. *Gaussian 98*; Gaussian, Inc.: Pittsburgh, PA, 1998.

(31) Calculated for the UHF structure using a Natural Population Analysis: Glendening, E. D.; Badenhoop, J. K.; Reed, A. E.; Carpenter, J. E.; Bohmann, J. A.; Morales, C. M.; Weinhold, F. *NBO 5.0*; Theoretical Chemistry Institute, University of Wisconsin: Madison, WI, 2001, as implemented in Gaussian 98.[30]

(32) The presence of diffuse functions is also not required for this result. At UHF/6-31G(d), the C_S structure is 6.9 kcal/mol more stable than the C_{2v} one, although the CN bonds are not as different in length, 1.361 and 1.399 Å.

(33) (a) Glendening, E. D.; Badenhoop, J. K.; Weinhold, F. *J. Comput. Chem.* **1998**, *19*, 593. (b) Glendening, E. D.; Badenhoop, J. K.; Weinhold, F. *J. Comput. Chem.* **1998**, *19*, 610. (c) Glendening, E. D.; Badenhoop, J. K.; Weinhold, F. *J. Comput. Chem.* **1998**, *19*, 628.

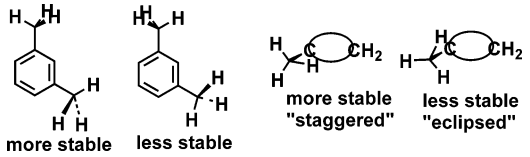

Figure 5. *m*-Xylene rotamers.

more stable than that eclipsed with the longer bond (C_1C_6, closer to C−C), as shown at the left of Figure 5. This is usually rationalized using the "two-membered ring" formulation of a double bond, where it may be seen that the out-of-plane CH bonds have a staggered relationship with the double bond orbitals in the more stable isomer, but are "eclipsed" in the less stable one.

The above calculations show the *m*-dinitrobenzene radical anion to be unsymmetrical in the gas phase, with the symmetrical structure apparently being a conical intersection, although detailed work on this question has not been carried out yet. It is thus a Class II intervalence compound, for which Marcus−Hush theory was designed. Unfortunately, there is a great deal of spin contamination in the above calculations, $S^2 > 1.2$ for both the UHF and the UMP2 structures, so these calculations do not address the spin distributing in these compounds, which is the principal experimental information available. One way around what Bally and Borden call "The Scylla of Spin Contamination"[27b] problems is to employ multiconfigurational approaches, but all that we know of that use large basis sets are dauntingly expensive and do not allow geometry optimization using modeled solvent, so that the effect of solvent on the geometry, which is expected to be crucially important for **1**$^{\bullet-}$, could not be modeled. We have currently stopped trying to make large basis set calculations work for these difficult systems. Even larger spin contamination was obtained upon attempts at accounting for solvent using the conductor-like screening model" (COSMO) polarizable continuum dielectric model[34] implemented in Gaussian 98. Note in this context that using diffuse-augmented basis sets is not appropriate for condensed-phase calculations unless a constraining potential is used, a factor not considered in COSMO calculations. One way around this problem is to use the "boxed-electron method",[35] which simply involves limiting the extent of the most diffuse basis functions. This technique is, however, relatively arbitrary and cannot be relied upon to give quantitative results.

We have instead carried out semiempirical AM1 calculations[36] that allow geometry optimization, using singles-only configuration interaction (CIS) including all MOs (70 valence orbitals in AM1). These calculations used the development version of VAMP 9.0 under Windows.[37] Geometries were fully optimized using the COSMO solvent model to a gradient norm of 0.4 kcal/mol. The symmetrical C_{2v} structure proves to be a transition state for these calculations, and, to obtain a symmetrical wave function, the reference wave function was calculated by distribution of the single unpaired electron over two molecular orbitals using the half-electron approximation (keyword OPEN(1,2)).[38] Thus, the energies of the symmetrical and unsymmetrical species are slightly different (by 0.1 kcal/mol, see Supporting Information, Table S1), even in vacuo, because different reference wave functions were needed for the two species. Figure 6 shows the heats of formation as a function of the Kirkwood solvent parameter, $(\epsilon_s - 1)/(2\epsilon_s + 1)$, where ϵ_s is the static dielectric constant. Although the enthalpy of the symmetrical transition state remains linear with the Kirkwood parameter, the unsymmetrical ground state curves downward as ϵ_s increases. These calculations provide an excellent example of quantification of Water's and co-workers' prediction of preferential solvent stabilization.[8d] Also shown in Figure 6 is the barrier to ET, calculated as the enthalpy difference, $\Delta H_f(C_{2v}) - \Delta H_f(C_1)$. These calculations find the C_{2v} species to be a transition state, and not an intermediate on the energy surface for ET, and are thus consistent with the success of the Marcus−Hush treatment of the optical data. The geometry changes that lead to the heat of formation changes shown in Figure 6 are considered in Figure 7. The nitrogens remain planar upon increasing ϵ_s, but the C−N and N−O bond lengths change significantly.[39] The largest changes occur at the NO_2 that bears most of the extra charge, the C−N bond length decreases by 0.05 Å and the N−O bond lengths increase by 0.03 Å (shown using the solid lines), while the other NO_2 has smaller changes in the opposite direction, C−N increase by 0.015 Å and N−O decrease by 0.005 and 0.002 Å (shown using dashed lines). Almost all of the geometry change occurs by $\epsilon_s = 10$. The unsymmetrical geometries resemble the UHF and UMP2 gas-phase geometries.

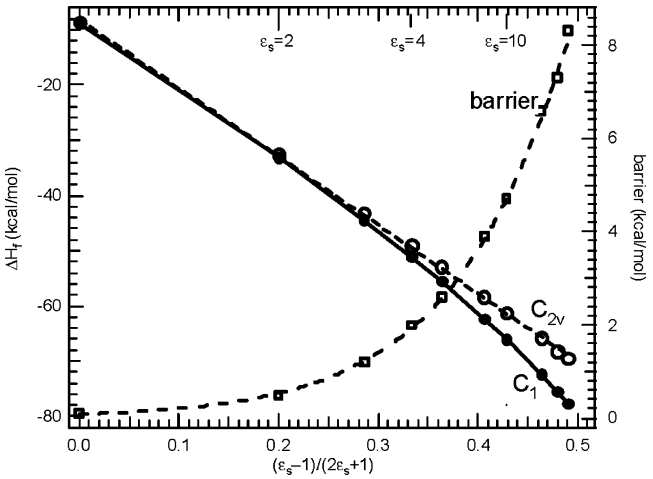

Figure 6. The calculated (AM1, CIS, 70 active orbitals, COSMO, fully optimized) heats of formation (left axis) for the unsymmetrical (C_1) and symmetrical (C_{2v}) structures of **1**$^{\bullet-}$, plotted against the Kirkwood parameter, $(\epsilon_s - 1)/(2\epsilon_s + 1)$. The squares (right axis) show the barrier calculated as the difference in heat of formation of the two structures.

(34) Klamt, A.; Schüürmann, G. *J. Chem. Soc., Perkin Trans. 2* **1993**, 799.
(35) Clark, T. J. C. S. *Faraday Discuss.* **1984**, *78*, 203. Guerra, M. *J. Phys. Chem. A* **1999**, *103*, 5983.
(36) (a) AM1 calculations: Dewar, M. J. S.; Zoebisch, E. G.; Healy, E. F.; Stewart, J. J. P. *J. Am. Chem. Soc.* **1985**, *107*, 3902. (b) Holder, A. J. In *AM1, Encyclopedia of Computational Chemistry*; Schleyer, P. v. R., Allinger, N. L., Clark, T., Gasteiger, J., Kollman, P. A., Schaefer, H. F., III, Schreiner, P. R., Eds.; Wiley: Chichester, 1998; p 8.
(37) Clark, T.; Alex, A.; Beck, B.; Burkhardt, F.; Chandrasekhar, J.; Gedeck, P.; Horn, A. H. C.; Hutter, M.; Martin, B.; Rauhut, G.; Sauer, W.; Schindler, T.; Steinke, T. *VAMP 9.0*; Erlangen, 2003.
(38) Clark, T. *A Handbook of Computational Chemistry*; Wiley: New York, 1985; p 85.
(39) In contrast, when spin contamination is removed by quartet annihilation after each SCF cycle (keyword AUHF in VAMP), both COSMO calculations and those in the presence of three or more judiciously placed waters on dinitroaromatics also produce a charge localization at ϵ_s of about 10, but get an entirely different geometry change. In these calculations, the negatively charged nitrogen becomes pyramidal and loses its barrier for twisting. Because the nitrogen ESR splitting is very sensitive to s hybridization, and the large nitrogen splitting of **1**$^{\bullet-}$ is no larger than that of nitrobenzene radical anion, we do not believe that this predicted geometry can be correct, and we will not consider these calculations further.

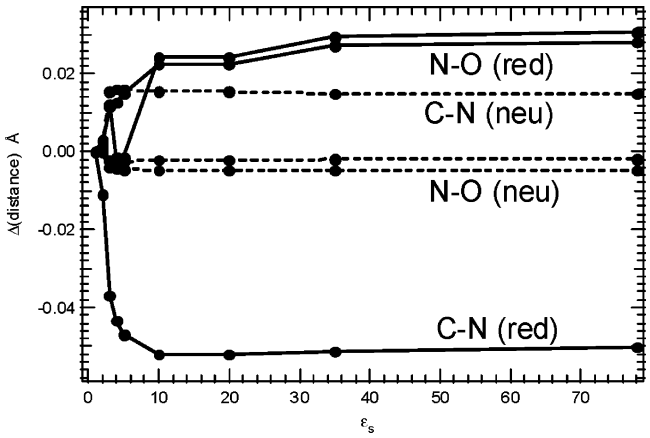

Figure 7. Changes in nitro group CN and NO bond lengths as ϵ_s is increased. Those at the nitro that take most of the negative charge are connected with solid lines, and those at the other nitro group are connected with dashed lines.

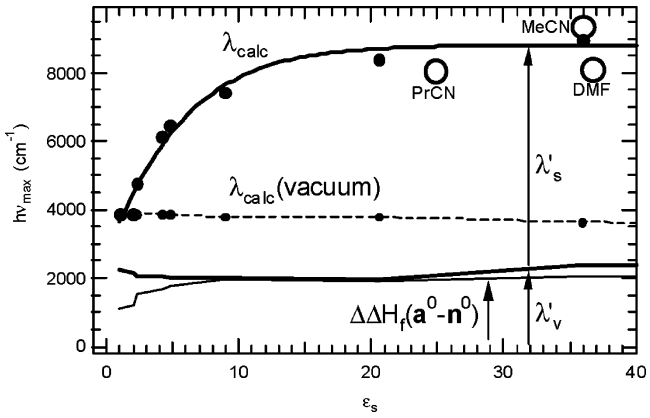

Figure 8. The calculated (AM1, CIS, 70 active orbitals, PCM-SCRF) vertical excitation energy λ_{calc} including both solvent and vibrational components (upper solid line) and vibrational component λ_v (lower solid line) for $\mathbf{1}^{\bullet-}$ as a function of the solvent static dielectric constant. See text for $\Delta\Delta H_f(\mathbf{a}^0 - \mathbf{n}^0)$ and λ_{calc}(vacuum).

Single-point calculations to determine the vertical reorganization energy λ_{calc} used our polarizable continuum model self-consistent reaction field (PCM-SCRF) technique,[40] with the modifications introduced by Gedeck and Schneider for non-equilibrium solvation,[41] and without a dispersion correction. λ_{calc} is the lowest doublet-to-doublet transition energy allowing only electronic polarization of the solvent. The Supporting Information, Table S2, compares λ_{calc} with values including complete solvent relaxation and "fluorescence" (solvent relaxed for the excited state), which are of interest in other contexts. The dependence of λ_{calc} and its internal vibrational and solvent reorganization components λ_v' and λ_s' upon ϵ_s are compared with the optically measured λ in three solvents in Figure 8. Although ϵ_s is not the only factor that affects experimental λ values, the λ_{calc} values obtained in this work compare well with the experimental transition energies. The vibrational component λ_v' was calculated from heats of formation for the neutral, anion, and their vertical species with alternate charge, as we introduced earlier.[42] If the geometry of the relaxed anion is designated **a**, that of the relaxed neutral is designated **n**, and the charges calculated are shown as superscripts 0 and −1, $\lambda_v' = \Delta\Delta H_f(\mathbf{a}^0 - \mathbf{n}^0) + \Delta\Delta H_f(\mathbf{n}^{-1} - \mathbf{a}^{-1})$. As indicated by the thin lowest line in Figure 8, although the first term, $\Delta\Delta H_f(\mathbf{a}^0 - \mathbf{n}^0)$, increases monotonically as ϵ_s increases because the geometry change increases, there is a partially compensating decrease in the second term, $\Delta\Delta H_f(\mathbf{n}^{-1} - \mathbf{a}^{-1})$, and the total λ_v' only varies slightly. By far, the largest component of λ_{calc} in polar solvents is λ_s'. Also shown in Figure 8 is λ_{calc}(vacuum), the lowest doublet-to-doublet excitation energy for structures having the optimized geometries, but calculated for a vacuum (at $\epsilon_s = 1$), shown as the dashed line at nearly constant values. This does not correspond to λ at any ϵ_s because charge is always calculated to be delocalized (but unsymmetrical when the structure is unsymmetrical) in the absence of solvent, so this number corresponds to calculated $2H_{ab}$, not to a λ. Because λ is calculated to exceed $2H_{ab}$ even at low dielectric constant, charge localization occurs rapidly as ϵ_s increases above 1, as indicated both by the geometry change (Figure 4) and by the λ value (Figure 8) plots. We note that the H_{ab} obtained as $^1/_2\lambda_{calc}$(vacuum) is almost 6 times as large as that obtained from the optical spectrum using a d_{12} near that of the N,N distance (see Table 2).

Conclusions

The dinitroaromatic anion $\mathbf{1}^{\bullet-}$ does not provide a simple model for electron hopping ET. Intramolecular ET rate constants for $\mathbf{1}^{\bullet-}$ are predicted within an order of magnitude by a Marcus−Hush-type two-state classical model analysis of the optical spectrum, which precludes the symmetrical bridge-reduced species as an intermediate having an energy minimum in the transfer of an electron between the two nitro groups. Because charge is largely localized on one nitro group, and simple two-state Marcus−Hush theory works well, it is appropriate to describe the system using Marcus−Hush language. The effective λ must be greater than $2H_{ab}$, and, to achieve a high λ, there must be a geometrical difference between the neutral and reduced nitro groups (although it could in principle just be in the solvent shell). UHF and MP2 calculations with a 6/31+G-(d) basis set give a planar, unsymmetrical gas-phase structure for $\mathbf{2}^-$, although spin-contamination renders these results unreliable and they may in any case not be appropriate for condensed phases. Although gas-phase AM1 calculations obtain a symmetrical minimum energy structure, COSMO calculations demonstrate a rapid increase in calculated reorganization energy as the solvent dielectric constant is increased.

Experimental Section

Commercial **1** was purified as previously described.[9c]

Preparation of Samples. Radical anions were prepared in vacuum-sealed glass cells equipped with an ESR tube and a quartz optical cell. The concentration of the samples (1−2 mM) was determined spectrophotometrically before reduction using the 360 and 350 nm bands of **1**. A 100 times excess of **3** was used. Reduction was achieved by contact with 0.2% Na−Hg amalgam.

ESR Fitting Procedure. The ESR splitting constants used in the simulations were adjusted for best fit to each spectrum. A fixed value of 0.2 G was used for the nitrogen splitting constant of the less solvated nitro group. This is close to the experimental value obtained for dinitroaromatic radicals in alcohols, where the electron transfer is slow enough that different splitting constants for the two nitrogen atoms can be measured. The two smaller hydrogen splittings are small enough that the same values could be used without affecting the calculated

(40) Rauhut, G.; Clark, T.; Steinke, T. *J. Am. Chem. Soc.* **1993**, *115*, 9174.
(41) Gedeck, P.; Schneider, S. *J. Photochem. Photobiol., A* **1997**, *105*, 165.
(42) Nelsen, S. F.; Blackstock, S. C.; Kim, Y. *J. Am. Chem. Soc.* **1987**, *109*, 677.

spectra detectably, but the nitrogen and larger hydrogen splittings (H_1 and H_8) were both adjusted for best fit. It was assumed that both splittings have the same sign for both a(N) and $a(H_{1,8})$, although this is not rigorously known.

Supporting Information Available: A list of additional references to dinitro anion ESR studies, fitted exchange rate constants as a function of temperature in acetonitrile, dimethylformamide, and butyronitrile, along with the ESR splitting constants used at the extreme temperatures and three examples of experimental and fitted ESR spectra. Tables of the data plotted in Figures 3 and 5. This material is available free of charge via the Internet at http://pubs.acs.org.

JA046566V